Interpretation of hydrocarbon plume biodegradation in 2-D bench-scale tank experiments by reactive transport modelling

CHRISTOF BEYER[1], ELISABETTA BALLARINI[1], ROBERT D. BAUER[2], CHRISTIAN GRIEBLER[2], SEBASTIAN BAUER[1]

1 Institute of Geosciences, University of Kiel, Ludewig-Meyn-Str. 10, D-24118 Kiel, Germany
cb@gpi.uni-kiel.de

2 Helmholtz Zentrum München, Institute of Groundwater Ecology, Ingolstaedter Landstr. 1, D-85764 Neuherberg, Germany

Abstract High resolution reactive transport modelling was applied as a tool for a model-based interpretation of detailed laboratory experiments on the interplay of transverse mixing and aerobic and anaerobic hydrocarbon biodegradation. As a typical groundwater contaminant, ethylbenzene (as a mixture of unlabelled and fully deuterium-labelled isotopologues) was continuously injected into a 2-D bench-scale flow-through tank through a central inlet port, generating a hydrocarbon plume along the whole length of the tank. During the first phase of the experiment, where the tank was recharged with water containing oxygen as the major dissolved electron acceptor, the aerobic strain *Pseudomonas putida* F1 was inoculated in order to initiate aerobic biodegradation of the ethylbenzene. Later, nitrate was added as an additional electron acceptor and the denitrifying strain *Aromatoleum aromaticum* EbN1 was inoculated to study competitive degradation under aerobic / anaerobic conditions. The spatial distribution of anaerobic degradation was investigated using measurements of compound-specific stable isotope fractionation along a vertical profile at the tank outlet. The numerical model was calibrated to fit the measured concentration profiles of these compounds at the outlet ports. Simulated and measured ethylbenzene and oxygen concentrations showed a good agreement for the aerobic degradation phase of the experiment, while the evaluation of the aerobic/anaerobic phase with competitive biodegradation was ambiguous due to uncertainties regarding the actual stoichiometry of the specific denitrification reaction. The model results, calibrated on the stable isotope signatures, showed that for the case of aerobic/anaerobic degradation the observed isotopic pattern strongly depends on the assumed initial distribution of microbial biomass.

Key words hydrocarbon biodegradation; isotope fractionation; numerical modelling; transverse dispersion

INTRODUCTION

The natural attenuation of oxidizable organic contaminants like BTEX in groundwater through biodegradation depends on the presence of compatible microbial communities and sufficient amounts of electron acceptor. Theoretical (e.g. Cirpka *et al*., 1999) as well as empirical studies (e.g. Bauer *et al*., 2008) have shown, especially for LNAPL hydrocarbon plumes, that biodegradation mostly takes place along the plume fringe, where diffusion and transverse dispersion induce the mixing of dissolved electron acceptors into the contaminant plume. A series of well-controlled reactive transport experiments in homogeneous and heterogeneous porous media has been performed by Bauer *et al*. (2009) in order to analyse the influence of transverse mixing on aerobic and anaerobic biodegradation. In Bauer *et al*. (2009) a combination of numerical and steady state analytical reactive transport modelling has been applied. Here, we present results of a model based evaluation of one of these experiments using numerical transient reactive transport modelling, which allowed for the simulation of the temporal development of microbial growth and contaminant biodegradation in the experiment.

METHODS

Flow-through tank experiment

The work presented in this paper is based on a 74-day reactive transport experiment, which is presented in detail in Bauer *et al*. (2009). The flow-through glass tank used for the experiment has inner dimensions of 77.3 cm length, 14 cm height and 1.1 cm width and was filled with sterile quartz sand with an average diameter of 0.25 mm. Saturated flow through the porous medium was

established by injection of groundwater containing oxygen (270 µmol L^{-1}) and nitrate (112 µmol L^{-1}) through 10 inlet ports (1 mm inner diameter) vertically spaced at 1.2 cm intervals along the left hand side of the tank, and simultaneous extraction from 10 outlet ports along the right hand side, resulting in an average transport velocity of 1.2 m d^{-1}. The experiment started with the injection of toluene at a concentration of 50 µmol L^{-1} through the 4th port from the top (phase I). For this port nitrate concentrations were reduced to 94 µmol L^{-1}. Simultaneously, the aerobic strain *Pseudomonas putida* F1 was inoculated through adjacent ports 3 and 5. Toluene concentrations were successively raised over a period of 36 days up to a value of 210 µmol L^{-1} (phases II–VI). On day 37 toluene was substituted by ethylbenzene as the carbon source (200 µmol L^{1}) injected as a 3:1 mixture of unlabelled and fully deuterium-labelled isotopologues ($C_8{}^1H_{10}$, $C_8{}^2H_{10}$) (phase VII). On day 46 nitrate concentrations in the groundwater of ports 1–3 and 5–10 were raised to 1316 µmol L^{-1} and the anaerobic denitrifying strain *Aromatoleum aromaticum* EbN1 was additionally inoculated (phase VIII), in order to study the competitive aerobic / anaerobic degradation of ethylbenzene. Monitoring data included regular measurements of ethylbenzene and nitrate concentrations at the outlet ports, as well as non-invasive optode-array measurements of vertical oxygen profiles using oxygen sensitive membrane foils (Microx 1 / FIBOX, PreSens, Regensburg, Germany) attached to the inner tank wall at distances of 40, 57 and 74 cm from the inlet. For ethylbenzene, ratios of $C_8{}^1H_{10} : C_8{}^2H_{10}$ were determined at selected sampling dates.

Numerical model

The OpenGeoSys code (OGS; Kolditz & Bauer, 2004; Kolditz & Shao, 2009) was applied for the simulation of the experiment. The code has been used e.g. by Ballarini *et al.* (2010), for the simulation of conservative tracer transport experiments related to the tank experiment presented in this paper. OGS solves the groundwater flow and transport equations by standard Galerkin finite element methods and using semi-implicit finite differences for the time derivatives. Kinetic growth of microbial populations coupled to the consumption of substrates is simulated using an operator splitting concept. MPI parallelization allows the decomposition of the finite element mesh into sub-domains, which can be distributed to individual processors of a high performance parallel computer (Wang *et al*., 2009). For kinetic reactions, the systems of coupled differential equations describing reactions at individual mesh nodes are independent from each other and hence can be distributed to the multiple processors of the parallel computer to be solved simultaneously.

In OGS general growth kinetics of a microbial species X (M L^{-3}) on several substrates (electron donors or acceptors) are described by multiple Monod equations. For isotope fractionation of ethylbenzene degraded in the experiment by *A. aromaticum* EbN1 (X_A), where the electron donor is injected as a mixture of isotopologues $C_8{}^1H_{10}$ and $C_8{}^2H_{10}$, the growth equation consists of contributions from both isotopologues (VanBreukelen & Prommer, 2008):

$$\frac{\partial X_A}{\partial t} = \mu_{\max} X_A \frac{NO_3^-}{M_{NO_3^-} + NO_3^-} \frac{C_8{}^1H_{10}}{M_{C_8H_{10}} + C_8H_{10}} \frac{I_{X_A}}{I_{X_A} + X_A} + \mu_{\max} X_A \frac{NO_3^-}{M_{NO_3^-} + NO_3^-} \frac{C_8{}^2H_{10}}{M_{C_8H_{10}} + C_8H_{10}} \frac{I_{X_A}}{I_{X_A} + X_A} \left(1 + \frac{\varepsilon}{1000}\right) - \xi X_A \quad (1)$$

where t is time (T), μ_{max} (T^{-1}) is the maximum growth rate of the microbial population, NO_3^- and C_8H_{10} are nitrate and total ethylbenzene concentrations (M L^{-3}), respectively, $C_8{}^1H_{10}$ and $C_8{}^2H_{10}$ are concentrations of the respective isotopologues (M L^{-3}), M_{NO3-} and M_{C8H10} are nitrate and ethylbenzene Monod concentrations, ε is the kinetic isotopic enrichment factor (-) and ξ (T^{-1}) is a first order rate coefficient describing bacterial decay. $I_X / (I_X + X)$ is a capacity term, which limits microbial growth beyond a certain size of the population I_X (M L^{-3}). Note that inhibition of *A. aromaticum* EbN1 growth by oxygen is not included here. According to equation (1), $C_8{}^1H_{10}$ and $C_8{}^2H_{10}$ are simulated as two different reactive species. For aerobic degradation of ethylbenzene by *P. putida* F1 (X_P), which does not discriminate between $C_8{}^1H_{10}$ and $C_8{}^2H_{10}$, equation (1) reduces to:

$$\frac{\partial X_P}{\partial t} = \mu_{\max} X_P \frac{O_2}{M_{O_2} + O_2} \frac{C_8H_{10}}{M_{C_8H_{10}} + C_8H_{10}} \frac{I_{X_P}}{I_{X_P} + X_P} - \xi X_P \quad (2)$$

where O_2 and M_{O2} are the oxygen and the corresponding Monod concentrations (M L^{-3}). The consumption of substrates S_i (electron donors and acceptors) is coupled to equation (1) or (2) via:

$$\frac{\partial S_i}{\partial t} = \frac{-St_i}{Y_C} \left[\frac{\partial X}{\partial t} \right]_{growth} \quad (3)$$

where Y_C (M_{cell} $M_{substrate}^{-1}$) is the yield coefficient for the electron donor and St_i [-] is the stoichiometric coefficient for substrate S_i of the electron donor/acceptor specific reaction equation. Note that in equation (3) for $C_8{}^1H_{10}$ and $C_8{}^2H_{10}$ and nitrate reduction only the isotopologue specific contribution to growth of equation (1) is evaluated, respectively.

Parameterization

The numerical evaluation of the experiment was focused on phases VII and VIII, where the electron donor toluene was replaced by ethylbenzene, i.e. for $t > 36$ days. A 2D finite element mesh of 89 902 nodes was created. The mesh was refined around the injection ports and along the plume region in order to minimize numerical dispersion, which is critical in the numerical simulation of mixing limited reactions. Accuracy of the numerical simulations was verified against analytical solutions and by grid refinement tests. Hydraulic conductivity K of the tank was set to a value of 4.11×10^{-4} m s^{-1}. A porosity n of 0.40 (-), longitudinal and transverse vertical dispersivities α_L and α_T of 7.6×10^{-4} and 7.6×10^{-5} m were determined from tracer test data. Parameters of the Monod models for growth of the microbial populations, which were determined experimentally as well as by model calibration or taken from literature data (cf. Bauer *et al*., 2008, 2009), are summarized in Table 1. Reaction stoichiometries for aerobic and anaerobic ethylbenzene degradation are given by equations (4) and (5).

$$C_8H_{10} + 10.5O_2 + 3H_2O \rightarrow 8HCO_3^- + 8H^+ \quad (4)$$

$$C_8H_{10} + 21NO_3^- + 3H_2O \rightarrow 8HCO_3^- + 21NO_2^- + 8H^+ \quad (5)$$

Table 1 Parameters for kinetically limited growth of the microbial strains on ethylbenzene.

Parameter	Symbol	Unit	*P. putida* F1	*A. aromaticum* EbN1
maximum growth rate [a]	μ_{max}	s^{-1}	$1.52 \cdot \times 10^{-4}$	$1.34 \cdot \times 10^{-5}$
decay rate [b]	ζ	s^{-1}	$-1.16 \cdot \times 10^{-6}$	$-1.16 \cdot \times 10^{-6}$
Monod conc. for electron donor [a]	M_{C8H10}	µmol L^{-1}	10	11.4
Monod conc. for electron acceptor [c]	M_{O2}; M_{NO3-}	µmol L^{-1}	3	70
capacity of X_i [b]	I_{XP}; I_{XA}	µmol L^{-1}	100	1000
isotopic enrichment factor [a]	ε	–	0	–545.7

[a] measured; [b] calibrated; [c] taken from literature.

Neumann type boundary conditions of specified flow were used to reproduce the pumping rate at inlet and outlet ports, while the bottom and top of the tank were treated as no flow boundaries. Injection of NO_3^-, O_2 and C_8H_{10} according to the experimental conditions (see above) was represented by Dirichlet type boundary conditions of fixed concentrations at the individual injection ports. As initial conditions, O_2, NO_3^- and *P. putida* F1 distributions obtained from numerical simulations of the first 36 days of the experiment (phase I-VI) were used.

RESULTS

In Fig. 1 exemplary results of the numerical evaluation of the aerobic phase VII (days 37–46) are shown, where the electron donor was switched from toluene to ethylbenzene. Regarding the

ethylbenzene concentrations at the tank outlet, it must be noted that the measured data at the tank outlet increased at the end of the aerobic period, while the numerical model reached steady-state after a few days. Nevertheless, the numerical results corresponded well with the last measurements of ethylbenzene between days 44 and 46 (Fig. 1(a)). Also, the measured oxygen distribution was well reproduced by the numerical simulations as can be seen exemplarily for the profile at the oxygen sensitive foil 40 cm from the tank inlet (Fig. 1(b)).

Figure 2 shows the simulated distribution of *P. putida* F1 biomass. The aerobic ethylbenzene degraders grew preferentially close to the inlet, where oxygen and ethylbenzene were both available at high concentrations, and along the fringe of the oxygen depleted ethylbenzene plume, where oxygen was provided by transverse mixing from the ambient groundwater. The simulated distribution is somewhat idealized and differs from the real situation in the experiment, where the biomass was found to have spread all over tank. In addition, the highest biomasses were observed at the fringes of the plume. The simulated distribution hence should be interpreted with care and as a measure of biomass activity rather than as an absolute amount.

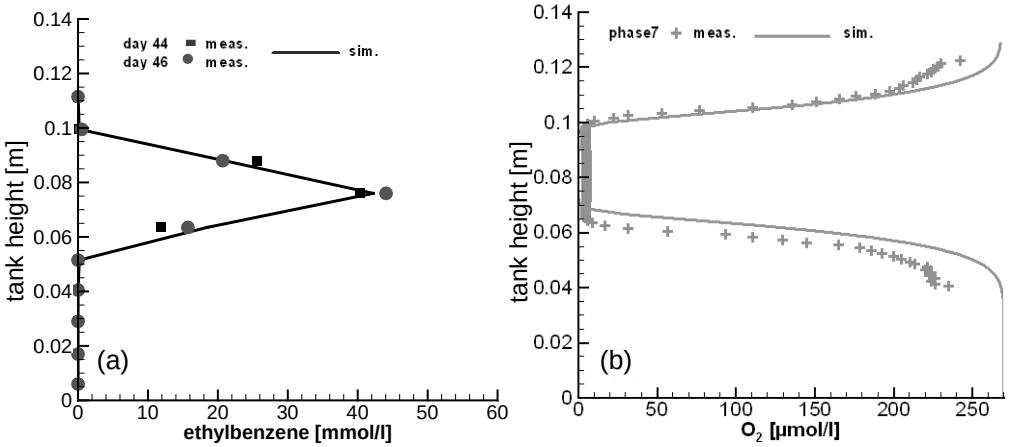

Fig. 1 Comparison of observed and simulated ethylbenzene at the outlet ports (a) and oxygen (b) concentrations 40 cm from the tank inlet during phase VII (measured oxygen concentrations are averaged over phase VII).

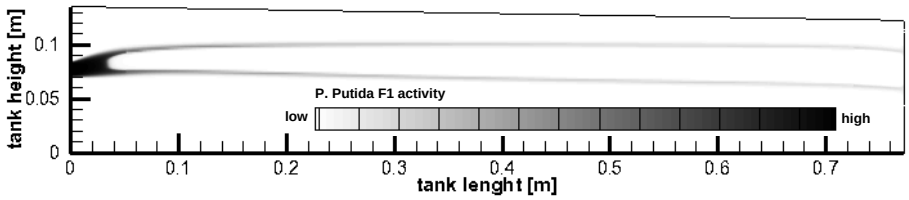

Fig. 2 Simulated *P. putida* F1 activity after 36 days of toluene and 9 days of ethylbenzene injection into aerobic groundwater.

On day 46 (phase VIII), the denitrifier *A. aromaticum* EbN1 was inoculated and nitrate concentrations in the groundwater medium were raised (see above). The spatial distribution of anaerobic degradation activity of *A. aromaticum* EbN1 was studied by analysing the distribution of ethylbenzene isotopologues $C_8{}^1H_{10}$ and $C_8{}^2H_{10}$ at the outlet ports on days 47, 51 and 53. Whereas *P. putida* F1 does not discriminate between the isotopologues, *A. aromaticum* EbN1 metabolizes the unlabelled substrate quicker than $C_8{}^2H_{10}$ which leads to enrichment of the latter in the undegraded residual fraction and hence in a shift of the ratio $C_8{}^1H_{10} : C_8{}^2H_{10}$. Figure 3 shows exemplary results from the numerical evaluation. A close reproduction of the measured data by the numerical model proved to be rather intricate. Especially, the simulated isotopic patterns were very

sensitive on the assumed distribution of the *A. aromaticum* EbN1 biomass after the inoculation. Ethylbenzene concentrations had already decreased during the first day after the inoculation, but did not reach a steady level during the observation period (Fig. 3(a)–(c)). The drop in ethylbenzene concentrations at day 47 was accompanied by a clear shift in isotopologue ratios (fractionation was not observed before day 47), which was strongest at the fringe of the plume (Fig. 3(d)). Ethylbenzene concentrations and isotopologue ratios remained on a rather constant level until day 52. On day 53 measured concentrations decreased considerably, which was accompanied by a decrease in isotopologue ratios at the plume fringes and in the core of the plume (Fig. 3(e),(f)). Ethylbenzene degradation increased further until the end of phase VIII (data not shown). For this period of the experiment, no further measurements of isotopologue ratios were taken.

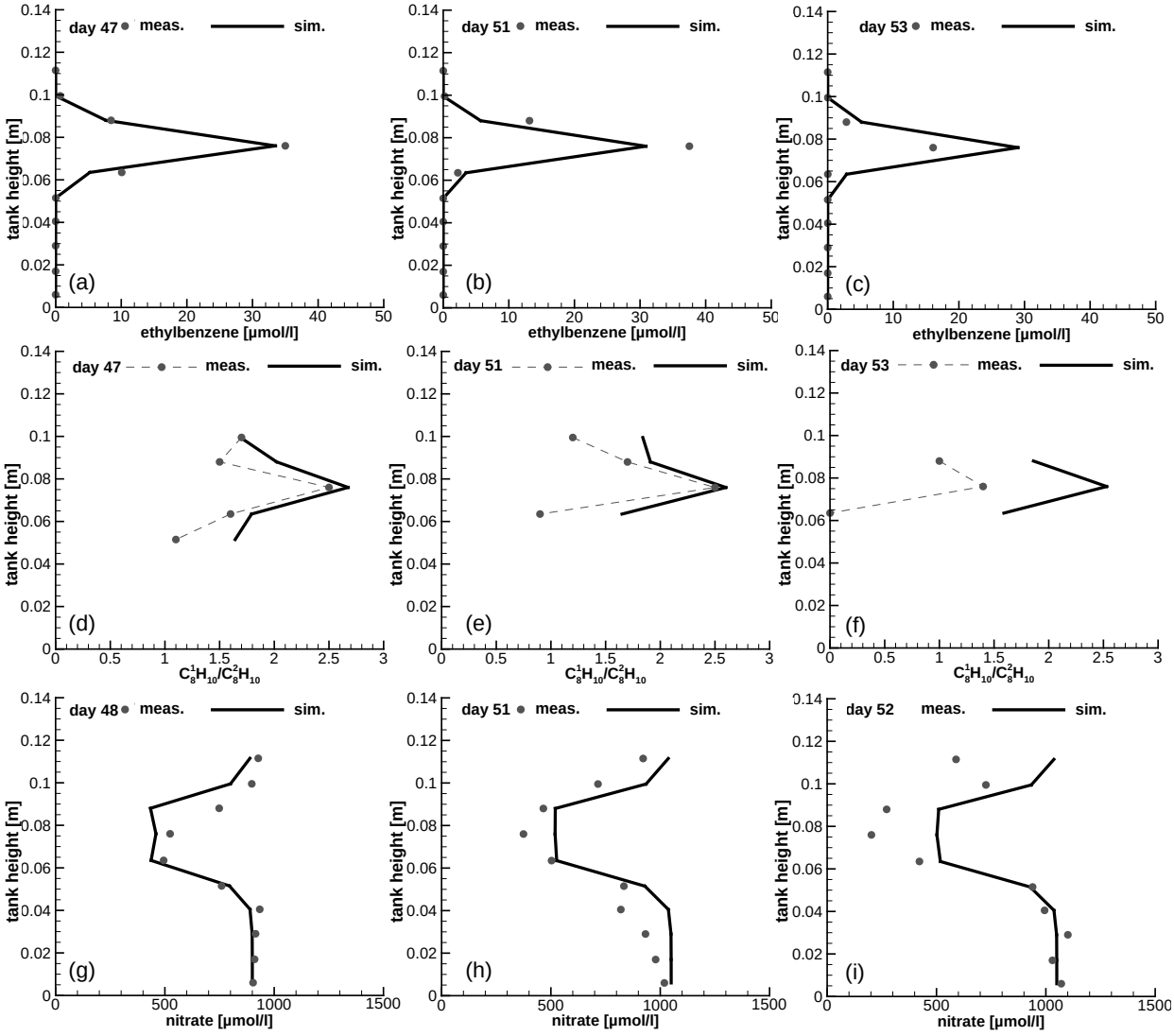

Fig. 3 Comparison of observed and simulated ethylbenzene concentrations ((a)–(c)), ratios of labelled and unlabelled ethylbenzene ((d)–(f)), and nitrate concentrations ((g)–(i)) measured at the outlet ports during phase VIII of the experiment.

First simulations, in which a uniform distribution of the *A. aromaticum* EbN1 biomass was used as initial condition for the experimental phase VIII, were not successful in reproducing the stronger shift in isotopic ratios at the plume fringe relative to the shift in the core of the plume. As nitrate concentrations throughout the tank were sufficiently high for a complete degradation of the

ethylbenzene plume, the biodegradation patterns obviously depend on the spatial distribution of the bacteria. As the microorganisms were inoculated through the two ports directly above and below the plume injection port, the spreading of the microbes from these ports into the tank was explicitly simulated in order to provide a more realistic distribution. Ethylbenzene concentrations predicted by the numerical model matched the measurements quite well for days 47 and 51. Similarly, comparison of measured and simulated nitrate concentrations (Fig. 3(g),(h)) showed a good agreement for days 48 (no nitrate measurements were taken on day 47) and 51. Also the simulated and measured isotopologue ratios showed a reasonably good reproduction of the general patterns (Fig. 3(d),(e)). The distinct increase in biodegradation dynamics between days 51 and 53, is obvious from the notable decrease of isotopologue ratios (Fig. 3(f)). However, ethylbenzene and nitrate concentrations (Fig. 3(c),(i)) were not captured by the model prediction.

SUMMARY AND CONCLUSIONS

In this paper, high resolution reactive transport modelling was applied as a tool for a model based evaluation of detailed laboratory experiments on competitive aerobic and anaerobic biodegradation of a 3:1 mixture of unlabelled and fully deuterated ethylbenzene isotopologues in a 2-D bench-scale flow-through tank. For the aerobic phase of the experiment, where the tank was recharged with water containing oxygen and the aerobic strain *P. putida* F1 was inoculated, simulated and measured ethylbenzene and oxygen concentrations showed a good agreement. For the aerobic / anaerobic phase, however, where nitrate was added as an additional electron acceptor and the denitrifying strain *A. aromaticum* EbN1 was inoculated, a good reproduction of the measured data by the numerical model proved to be intricate. The inoculation and spreading of *A. aromaticum* EbN1 biomass throughout the tank had to be explicitly simulated in order to reasonably reproduce the observed isotopologue ratios. Moreover, biodegradation dynamics showed a distinct change over time. During the first six days of the aerobic / anaerobic phase, ethylbenzene concentrations and isotopic ratios remained on a more or less constant level, which was reproduced well by the numerical model using a comparably low growth rate coefficient μ_{max} for *A. aromaticum* EbN1 (cf. Table 1). However, later on, anaerobic biodegradation notably increased, which so far could not be modelled satisfyingly without using a higher μ_{max}. It is hypothesized that the observed amount of anaerobic biodegradation during the first few days of the experimental phase is mainly due to the injected biomass and low growth dynamics, whereas the somewhat abrupt increase in biodegradation dynamics phase may be due to increased biomass growth after an adaptation to the system.

Acknowledgements This work is a cooperation within the research group “Reaction in porous media” (FOR 525/2) funded by the Deutsche Forschungsgemeinschaft.

REFERENCES

Ballarini, E., Bauer, S., Eberhardt, C., Rolle, M., Grathwohl, P. & Beyer, C. (2010) Design and evaluation of bench-scale tank experiments for the quantification of transverse dispersion using numerical simulations. In: *Groundwater Quality Management in a rapidly changing World.* (ed. by M. Schirmer, E. Hoehn, & T. Vogt). IAHS Publ. 342, IAHS Press, Wallingford, UK.

Bauer, R. D., Maloszewski, P., Zhang, Y., Meckenstock, R. U. & Griebler, C., (2008) Mixing-controlled biodegradation in a toluene plume - Results from two-dimensional laboratory experiments. *J. Cont. Hydrol.* 96, 150–168.

Bauer, R. D., Rolle, M., Bauer, S., Eberhardt, C., Grathwohl, P., Kolditz, O., Meckenstock, R. U. & Griebler, C. (2009) Enhanced biodegradation by hydraulic heterogeneities in petroleum hydrocarbon plumes. *J. Cont. Hydrol.* 105, 56–68.

Cirpka, O. A., Frind, E. O. & Helmig, R. (1999) Numerical simulation of biodegradation controlled by transverse mixing. *J. Cont. Hydrol.* 40, 159–182.

Kolditz, O. & Bauer, S. (2004) A process-oriented approach to computing multi-field problems in porous media. *J. Hydroinf.* 6(3), 225–244.

Kolditz, O. & Shao, H. (eds) (2009) Developer Benchmark Book on THMC Components of Numerical Codes GeoSys/Rockflow V. 4.9. Helmholtz Centre for Environmental Research (UFZ), Leipzig, Germany.

VanBreukelen, B. M. & Prommer, H. (2008) Beyond the Rayleigh equation: reactive transport modeling of isotope fractionation effects to improve quantification of biodegradation. *Environ. Sci. Technol.* 42(7), 2457–2463.

Wang, W., Kosakowski, G. & Kolditz, O. (2009) A parallel finite element scheme for thermo-hydro-mechanical (THM) coupled problems in porous media. *Computers & Geosciences* 35, 1631–1641.